

appear at 1416 and 1609 cm^{-1} characteristic respectively to symmetric and anti-symmetric vibration of COO^- of tartaric acid. The intensity of COO^- bands increases as function of acid concentration in solution and with zinc content, implying the formation of calcium and zinc tartarate on the hydroxyapatite surface. The NMR-MAS ^{13}C spectra of hydroxyapatite treated present two peaks at 74 and 181 ppm characteristic of two different carbons of tartaric acid. The formation of new hybrid compounds was confirmed by the shift of signals comparing with those of free tartaric acid. Moreover, the broadening of these peaks can be explained by the heterogeneity of carbon environment by the presence of zinc on the apatitic surface.

[1] T. Turki, A. Aissa, H. Agougui, M. Debbabi, *journal de la société chimique de tunisie*, **2010**, 12, 161-172.

Keywords: apatite, surface, fonctionnel

MS74.P16

Acta Cryst. (2011) A67, C676

How to deal with multiple solutions in powder pattern indexing

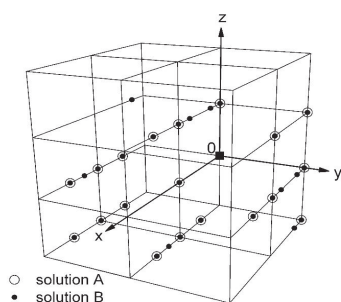
Rolf Heinemann, Diedrich Stöckelmann and Herbert Kroll, *Institut für Mineralogie, WWU Münster (Germany)*. E-mail: rhein_03@uni-muenster.de

Santoro et al (1980) [1] first addressed the question of equivalence when in powder pattern indexing more than one indexing solution and thus more than one reciprocal metric tensor are produced. Two metric tensors G_A^* and G_B^* are said to be equivalent when a matrix R exists such that $G_B^* = R G_A^* R^T$ (1). R is a 3×3 non-symmetric matrix consisting of rational numbers. Therefore, eq. (1) cannot be solved directly. Santoro et al (1980) [1] suggested to vary the elements of R systematically in the range (5, -5) until the equality sign in eq. (1) is fulfilled within chosen error limits.

We suggest a different procedure: First, the three shortest non-coplanar vectors that have the same Q values in both lattices A and B are identified. These vectors are taken to define a new basis common to A and B . Then, 3×3 matrices M_A and M_B are written which transform the axial systems of A and B into the new one. If the new axial system reproduces lattices A and B , then the equality $M_A G_A^* M_A^T = M_B G_B^* M_B^T$ (2) holds. Eq. (2) defines a new metric tensor common to both lattices A and B which we thus term the common metric tensor G_C^* . The coordinates of the reciprocal lattice points of A and B are transformed according to $(\eta/\kappa/\lambda)_{A,B} = (M_{A,B}^{-1})^T (h/k/l)_{A,B}$. Coincident lattice points yield $(\eta/\kappa/\lambda)_A = (\eta/\kappa/\lambda)_B$. If all lattice points coincide, lattices A and B are termed equivalent; if only a subset of points is coincident, the lattices are semi-equivalent; otherwise they are non-equivalent.

Equation (1) can be easily retrieved from equation (2): $G_B^* = M_B^{-1} M_A G_A^* M_A^T (M_B^{-1})^T = R G_A^* R^T$. Thereby we arrive at a solution to eq. (1) that avoids trial and error methods.

We take as an example two different indexing solutions A and B to $\text{CrPO}_4 \cdot 6\text{H}_2\text{O}$, given by Santoro et al. (1980) [1], to demonstrate the spatial relationship of the respective reciprocal lattice points. Fig. 1 shows that lattice points A and B coincide. However, solution A only explains a subset of points.



○ solution A
● solution B

[1] A. Santoro, A.D. Mighell, J.R. Rodgers, *Acta Cryst.* **1980**, A36, 796-800.

Keywords: powder pattern indexing, multiple solutions, metric tensor

MS74.P17

Acta Cryst. (2011) A67, C676

XRD and SAXS studies applied to doped Polyaniline and Poly(o-methoxyaniline)

Edgar Ap. Sanches,^a Juliana C. Soares,^a Graziella Trovati,^b Yvonne P. Mascarenhas,^a ^aUniversity of São Paulo (USP), Institute of Physics of São Carlos (IFSC), (Brazil). ^bUniversity of São Paulo (USP), Institute of Chemistry of São Carlos (IQSC), (Brazil). E-mail: edgar.sanches@ifsc.usp.br

Polyaniline (PANI) and derivatives of aniline have received great attention due to their technological applications. The introduction of polar functional groups and alkyl groups to the main chain of PANI is a practice to obtain soluble polymers in a wider variety of organic solvents. Poly(o-methoxyaniline) (POMA) is a derivative of PANI and its structural difference is the presence of the group ($-\text{OCH}_3$) in the *ortho* position of the carbon rings, been extensively studied in the form of powder or films for the most various applications. ES-PANI and ES-POMA were synthesized, respectively, according to the method described elsewhere [1,2] with times of synthesis ranging from 0,5 to 96 h. Samples were characterized by XRD, SAXS, LeBail Fit [3], SEM and van der Pauw method [4]. XRD analysis showed that the synthesis time was not significant in the crystallinity of PANI, however, it is an important parameter in the synthesis of POMA, which became more crystalline. LeBail Fit showed that the ES-PANI crystallites average size is 34 Å, while for ES-POMA the crystallites average size increases with increasing synthesis time (from 26 to 57 Å). By SAXS it was possible to obtain values of Radius of Giration (R_g) (217 Å for ES-PANI and 280 – 313 Å for ES-POMA); the maximum particle size (D_{max}) from the Pair-distance distribution Function ($p(r)$) (650 Å for ES-PANI and 900 Å for ES-POMA) and the particle organization qualitative analysis through Kratky curves, showing that for ES-PANI the crystallinity does not increase significantly over synthesis; for ES-POMA, particles became more ordered with increasing of crystallinity over the synthesis. Images of SEM allowed the visualization of different morphologies for PANI and POMA: while the PANI-ES showed fiber morphology formed by interconnected nanospheres, the POMA-ES had a globular vesicular morphology, which changed with increasing synthesis time. Conductivity measurements were not changed drastically in different synthesis time for ES-PANI ($1,84 \cdot 10^{-4} \text{S/cm}$), whereas for the ES-POMA the conductivity increased during the synthesis ($1,89 \cdot 10^{-7}$ to $8,89 \cdot 10^{-7} \text{S/cm}$). The results obtained by each of the techniques were essential to the understanding of the structure and properties of polymeric materials.

[1] S. Bhadra, N.K. Singha, D. Khastgir. *Journal of Applied Polymer Science* **2007**, 104, 1900–1904. [2] J.M. Yeh, C.P. Chin. *Journal of Applied Polymer Science* **2003**, 88, 1072–1080. [3] A. LeBail, H. Duroy, J.L. Fourquet. *Materials Research Bulletin* **1988**, 23, 447–452. [4] R. Robert, S.M. Berleze, *Revista Brasileira de Ensino de Física* **2007**, 29, 15-18.

Keywords: polyaniline, poly(o-methoxyaniline), XRD

MS74.P18

Acta Cryst. (2011) A67, C676-C677

The magnetic ordering in Mn_3TeO_6 and Co_3TeO_6

Roland Tellgren,^a Sergey Ivanov,^{ab} Per Nordblad,^b Roland Mathieu,^b

Clemens Ritter,^c Gilles André,^d ^a*The Angstrom Laboratory, Uppsala University, (Sweden)*. ^b*Karpov' Institute of Physical Chemistry, Moscow, (Russia)*. ^c*Institute Laue Langevin, Grenoble, (France)*. ^d*Laboratoire Léon Brillouin, CEN/Saclay, f-91191, Gif sur Yvette, (France)*. E-mail: rte@mkem.uu.se

Multiferroics have engendered increasing interest because of their many potential applications for micro- or nano-electronic devices, magnetic storage elements and interesting fundamental physics. The term "multiferroic" means coexistence of ferroelectric and magnetic ordering in a single phase or multiphase material. However, the two ordering parameters are mutually exclusive because ferroelectricity and magnetism require different filling states of the d-shells of transition metal ions. Empty d- shells mainly exist in ferroelectricity, while partially filled d-shells are required in magnetism. Therefore multiferroics are rare.

It exists several different microscopic mechanisms which may cause multiferroic behaviour . One of the most interesting is when a spontaneous polarization exists in a spiral or cycloidal magnetic structure. Accordingly, one strategy to find new multiferroic materials is to look for magnetic systems with that kind of magnetic structures.

The complex metal oxides Mn_3TeO_6 and Co_3TeO_6 have been prepared both as single crystals by chemical transport reaction and as polycrystalline powders by a solid state reaction route. The crystal structure and magnetic properties have been investigated using a combination of x-ray and neutron powder diffraction, electron microscopy, calorimetric and magnetic measurements. It has been shown that at room temperature Mn_3TeO_6 adopts a trigonal structure, space group R-3 ($a=8.8679(1)\text{\AA}$, $c=10.6727(2)\text{\AA}$) and Co_3TeO_6 the monoclinic spacegroup C 2/c ($a=14.7830(2)\text{\AA}$, $b=8.8395(1)\text{\AA}$, $c=10.3426(2)\text{\AA}$).

A long-range magnetically ordered state has been identified through variable temperature neutron diffraction and magnetic susceptibility measurements. The magnetic structure for the two compounds is very different. Mn_3TeO_6 has an incommensurate helix structure while Co_3TeO_6 shows a complicated but commensurate spin structure.

Keywords: neutron, ferroic, magnetism

MS74.P19

Acta Cryst. (2011) A67, C677

Thermal decomposition of ternary layered hydroxides

Stephane B.P. Farias,^a Luciano H. Chagas,^a Sandra S. X. Chiaro,^b Alexandre A. Leitão,^a Renata Diniz,^a ^a*Departamento de Química, Instituto de Ciências Exatas, UFJF, Juiz de Fora, (Brasil)*. ^b*Centro de Pesquisas da Petrobras (CENPES)* E-mail: stephane_farias@hotmail.com

Hydrotalcite are natural clays or synthetic defined as layered double hydroxides (LDH). These compounds exhibit various structural and chemical properties, besides having a high thermal stability, making them of great technological importance in obtaining new catalysts [1], [2].

Hydrotalcites samples containing Co, Mg and Al were subjected to increasing temperature in the range of 250-950 °C and measurements made X-ray diffraction in situ at Brazilian Synchrotron Light Laboratory (LNLS). The major changes occur between 250 and 400 °C, where the reflections of MgO begin to appear in X-ray diffraction (XRD) pattern. The XRD pattern reveals that the Mg-Al-Co hydrotalcite structure at 250 °C is not fully decomposed. It can be seen in relation to peaks in similar positions of the sample at room temperature, although only slightly wider and overlapped peak are observed. At temperatures above 400 °C the sample is completely decomposed and shows the disappearance of reflections at angles less than 30° indicating that the

structure of hydrotalcite collapsed during the calcination. In this stage occurs the formation of corresponding mixed oxides, a spinel mixture ($MgAl_2O_4$, Co_2MgO_4 , Al_2MgO_4), and overlapping peaks of oxides as Co_3O_4 . Between 400 and 600 °C, small variations are observed.

Calcination temperatures above 400 °C, occurs the Co^{2+} to Co^{3+} oxidizes forming phases Co_3O_4 , Co_2AlO_4 and $CoAl_2O_4$. All these compounds have cubic symmetry Fd-3m and it is not possible to distinguish one type of spinel phase from each other. At temperatures higher than 950 °C apparently is no longer observed any kind of modification.

A study was conducted to verify the regeneration capacity of the layered structure of hydroxides triple by simple exposure of the calcined material into the atmosphere where there is the presence of carbon dioxide and moisture. This material was characterized by X-ray diffraction. For this study, the calcined products performed at 800 °C and at 950 °C were calcined for one hour at each temperature. The samples were left in an inert atmosphere of nitrogen until the measurement of XRD was performed. Upon completion of the measurement, the samples were exposed to the atmospheric environment for 1 week and again performed the XRD measurements. It could prove the existence of two crystalline phases after calcination, attributed to a magnesium oxide and another characterized as spinel. The second phase is thermodynamically more stable and contributes to the broadening of diffraction peaks of the sample. The product of calcination showed a low-quality crystal, although there was a slight increase in the crystallinity of the material after exposure to the atmospheric. After exposure of the samples the air for one week there was no change in the diffraction pattern, indicating that calcination above 800 °C do not regenerate the layered structure of hydrotalcite therefore did not have the memory effect.

[1] E.L. Crepaldi, J. B. Valim, *Química Nova*, **1998**, 26, 300-311. [2] R.E. Johnsen, F. Krumeich, P. Norby, *Journal of Applied Crystallography*, **2010**, 43, 3, 434-447.

Keywords: hydrotalcite, powder X-ray diffraction, synchrotron radiation.

MS74.P20

Acta Cryst. (2011) A67, C677-C678

The reordering transition in layer disordered solids: Rare earth-transition metal intermetallic.

Pentón-Madrigal A,^a Estevez-Rams E,^b Somarriba J.C.,^b Lora Serrano R,^c ^a*Facultad de Física, Universidad de La Habana, San Lazaro y L. CP 10400. C. Habana (Cuba)*. ^b*Instituto de Ciencia y Tecnología de Materiales(IMRE), Universidad de La Habana, San Lazaro y L. CP 10400. C. Habana. Instituto de Física, Universidade Federal de Uberlandia, 38400-902 Uberlandia-MG, (Brasil)*. E-mail: arbelio@fisica.uh.cu

Planar faults are very frequently crystal defects. The quantification of this kind of defects has been the focus of attention since decades due to the fact that many alloys and compounds can be described as layer structures. The disruption of the periodicity in the stacking order leads to measurable effects in the profiles of the maxima of the diffraction pattern of a crystal. In this work, planar faulting is quantitatively studied beyond the model of independent faulting events [1], [2], [3] showing the strength of direct methods to extract defects information from the diffraction patterns [4], [5], [6]. The correlation length can be extracted from the diffraction data without need to assume the random faulting model by directly fitting the diffraction data. It is showed that the analysis of the decaying term of the probability correlation function, does not only allow quantifying the loss of memory in the system through the correlation length but also, the strength of interaction between faults. The behavior of the decaying terms turns